RILEM-*fib*-AFGC Int. Symposium on Ultra-High Performance Fibre-Reinforced Concrete,
UHPFRC 2013 – October 1-3, 2013, Marseille, France

EXPERIMENTS AND ANALYSIS OF SIZE AND SHAPE EFFECT OF UHPFRC SUBJECTED TO AXIAL AND FLEXURAL TENSION

Björn Frettlöhr (1), Karl - Heinz Reineck (2) and Hans - Wolf Reinhardt (3)

(1) EnBW Erneuerbare Energien GmbH, Hamburg, Germany

(2) ILEK,University of Stuttgart, Germany

(3) Department of Construction Materials, University of Stuttgart, Germany

Abstract

In order to analyse the size effect, several test series with two different UHPFRC were performed. Thereby identical cross sections were tested under bending and axial tension. Additionally the influence of the specimen shape (ratio width/height) was tested. The tensile tests showed a size effect and a shape influence for the elastic limit and for the tensile strength. This was critically analysed since some of the tested specimens had imperfections. Theoretical considerations based on optical fibre orientation measurements and a statistical analysis of the tensile tests concluded that possibly there is no size and no shape effect. The bending tests showed only a size effect for the elastic limit and a size and shape effect for the flexural tensile strength. Neither the theory of Weibull nor the empirical approach according to AFGC/SETRA (2002) could explain the test results. The fracture mechanics model by Frettlöhr (2011) could explain the experimentally determined size and shape influence of the flexural tensile strength. A comparison between the experiments and model exhibited low discrepancies.

Résumé

Afin d'analyser l'effet d'échelle, plusieurs séries d'essais ont été effectuées, avec deux BFUP différents, sur des échantillons à section identique soumis à des sollicitations de flexion et de traction pure. En outre, l'influence de la forme des échantillons (rapport entre largeur et hauteur) fut évaluée. Les essais de traction ont mis en évidence un effet d'échelle et une influence de la forme pour la limite élastique et pour la résistance à la traction. Ces phénomènes furent analysés de façon approfondie puisque certains échantillons contenaient des imperfections. Des considérations théoriques basées sur la mesure optique de l'orientation des fibres et sur une analyse critique des essais de traction ont montré qu'il n'existait probablement pas d'effet de forme ou d'échelle. Pour les essais de flexion, un effet d'échelle fut observé pour la limite élastique et un effet de forme et d'échelle pour la résistance à la traction par flexion. Les résultats des essais n'ont pu être expliqués ni par la théorie de Weibull, ni par l'approche expérimentale de la recommandation AFGC/SETRA (2002). C'est le modèle de mécanique de rupture de Frettlöhr qui a permis d'expliquer les influences de forme et d'échelle observées expérimentalement sur la résistance à la traction par flexion. Une comparaison entre les résultats d'essai et le modèle donne des écarts minimes.

1 MATERIAL CHARACTERISTICS OF UHPFRC

1.1 Strengths of control specimens

In the following a brief outline is given on the basic material characteristics of the Ultra High Performance Concrete (UHPC) used for their tests by Frettlöhr and Reineck (2009). For most tests the material was Ductal® G2 FM with a content of 2 % steel fibres delivered by Lafarge, Paris with steel fibres of the type Redaelli Tecna with Ø0,175 mm and l_f = 13 mm length. The test specimens were cast at the Otto-Graf-Institut, FMPA Stuttgart and were heat treated for 48 h at about 90°C in a water basin. The 59 compressive tests of cylinders (Ø100, h = 200 mm) yielded an average strength of f_{cm} = 211 MPa with a coefficient of variation of only v = 4,4 %. The modulus of elasticity in compression was on average E_{cm} = 53.071 MPa, and that under tension was E_{ctm} = 48.576 MPa and thus 8,5 % lower. The 99 flexural 4-point bending tests on control prisms 40 x 40 mm yielded the following average values for the tensile stress $\sigma_{ct,fl}$ = M/W: $f_{ctfl,el,m}$ = 21,6 MPa for the elastic limit with v = 12,5 %, and $f_{ctfl,m}$ = 42,3 MPa for the bending tensile strength with v = 8,9 %.

Additionally tests were performed with the material Duracrete Plus® delivered by Schwenk Zement AG, Ulm. The steel fibres were Stratec FM13/0.2 with Ø0.2 mm and l_f = 13 mm from the firm Stratec GmbH, Heme. The test specimens were cast by the firm Sebastian Wochner GmbH & Co.KG, Dormettingen and were heat treated as described above. The average compressive strength of 12 cylinders was f_{cm} = 168.6 MPa and the modulus of elasticity in compression was E_{cm} = 42.067 MPa, whereas that under tension was E_{ctm} = 38.247 MPa and thus 9 % lower. The flexural tests on the 21 control specimens yielded $\sigma_{ctfl,el}$ = 21.7 MPa and f_{ctfl} = 33.2 MPa.

1.2 Stress-strain curve in compression

The UHPFRC used exhibits a linear σ_c - ε_c - line almost up to the maximum strength as shown in Fig. 1 for the two materials with different concrete strengths.

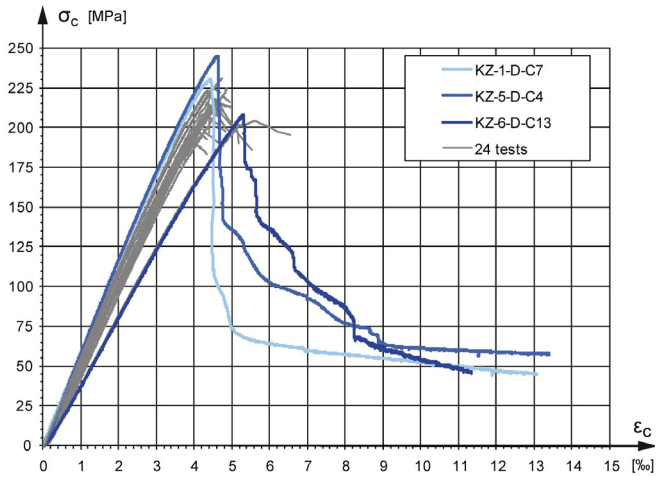

Figure 1: σ_c - ε_c – curves for deformation controlled compression tests with Ductal® on cylinders with Ø = 100 mm, h = 200 mm

The modulus of elasticity varies between E_{c0} = 47 and 58 GPa. In Fig. 1 many curves are plotted but only for 3 the descending branch could be measured. Very important is to note the

immediate steep decrease directly after the maximum stress is attained; this decrease is rather drastical and almost brittle down to a low level. Very similar results were obtained by Wefer (2010), who stated that the descending branch cannot be tested with sufficient security. Therefore, in design proposals the descending branch should be cautiously assumed, and especially any horizontal branch at the maximum strength is not justified by the real behaviour and is somehow deceiving as a stress-strain-curve for UHPFRC.

2 SIZE AND SHAPE EFFECT IN TENSION

2.1 Behaviour in tension

The typical behaviour for tests in axial tension is demonstrated in Fig. 2, where the axial tensile stress σ_{ct} = N/A is plotted versus the strain measured over a gauge length of 150 mm. For the evaluations special attention was paid to assess the axial tensile stress $\sigma_{ct,el}$ at the elastic limit and of course the maximum value of the axial tensile strength f_{ct}. All tests performed by Frettlöhr and Reineck (2009) exhibited a distinct stress increase after the elastic limit $\sigma_{ct,el}$ and in the range of micro-cracking before the axial tensile strength f_{ct} is attained, where localisation occurs. Therefore, the mean curves of all tests can be defined by the characteristic curve also shown in Fig. 2, which is defined by the values for $\sigma_{ct,el}$ and f_{ct}, a value of $f_{ct1} = \sigma_{ct,el} + 0{,}85\cdot(f_{ct} - \sigma_{ct,el})$ in between in the ascending branch, and four values in the descending branch.

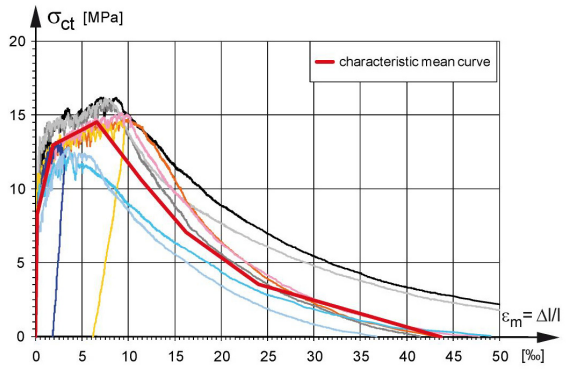

Figure 2: Stress-strain curves in axial tension of prisms h = 25 mm and b = 3·h = 75 mm (gauge length 150 mm)

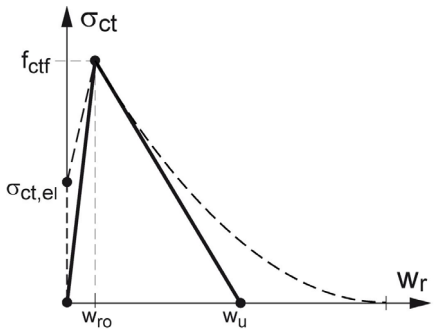

Figure 3: Relationship between the stress and the crack width and simplification

At the maximum stress f_{ct} localisation occurs and the stress decreases while fibres are pulled out in this descending branch. The strain measured over a certain gauge length is then governed by the crack width of the normally only one crack. Therefore, it is necessary to define this behaviour by a relationship between the stress and the crack width as shown in Fig. 3. Very often the dashed refined curve is simplified by the bilinear continuous line.

2.2 Results of the tests on the size and shape effect in axial tension

Different test series were performed to investigate the size effect (i.e. the decrease of strength with increasing height) and the shape effect (i.e. the decrease of strength with increasing width to height ratio b/h of prisms). The axial tensile stress $\sigma_{ct,el}$ at the elastic limit

as well as the tensile strength f_{ct} are each plotted versus the height h (Fig. 4 and Fig. 6) of the prisms as well as versus the ratio b/h (Fig. 5 and Fig. 7). In these figures the tests are shown in continuous lines and appear to exhibit a size effect as well as a shape effect of the prisms, as explained in more detail by Frettlöhr, Reineck and Reinhardt (2012). This was critically reviewed as explained in the following and the results are plotted in dashed lines in these Figs. 4 to 7.

2.3 Theoretical Considerations at the elastic limit

The behaviour at the elastic limit was compared with the theory of Weibull by Frettlöhr and Reineck (2009) and Reineck and Frettlöhr (2010, 2011). It turned out that the Weibull modulus m is not constant: for small volume ratios $\beta_v = V_2/ V_1 \leq 20$ values of up to m = 36 have to be applied whereas for $\beta_v > 20$ lower values in the range of m = 12 to 20. In summary, the theory of Weibull appears not to be valid for this case.

Since theoretically there is no explanation for both effects neither for the elastic limit nor for the tensile strength, the test results were critically re-examined by Frettlöhr (2011). The reason for this was that some of the larger test specimen had imperfections due to the specimen ends being slightly curved towards the upper side of the formwork. Furthermore some of the test specimen localised outside of the defined measurement range of the dog bone shaped specimens. Frettlöhr (2011) used a statistical approach to investigate the influence of these imperfections by forming different groups of the tests without and with imperfections. The tensile test specimens were divided into for groups:

Group 1: Specimens with localisation inside the measurement range and no imperfection;
Group 2: Specimens with localisation outside the measurement range and no imperfection;
Group 3: Specimens with imperfection;
Group 4: All specimens of Groups 1 and 2 without imperfection.

The ratio of the mean value $\sigma_{ct,el}$ at the elastic limit of Groups 1 and 2 gives an indication for the influence of the localisation place; this ratio is equal to 1.05 so that this influence can almost be neglected. Therefore the Groups 1 and 2 were combined to Group 4 and compared with Group 3. This exhibited that the specimens of Group 3 with imperfections reached only 78% of Group 4 without imperfections. Therefore, one can conclude that the mean value at the elastic limit $\sigma_{ct,el}$ of Group 3 could be estimated higher by 1/0.78.

In Fig. 4 the mean value of the elastic limit $\sigma_{ct,el}$ of the tests is plotted versus the specimen height h, and in Fig. 5 $\sigma_{ct,el}$ is plotted versus the shape ratio width to height b/h. For comparison with the original test results (shown in continuous lines) also the 1/0.78 times higher estimated values of Group 3 are shown as dashed lines.

It can be seen that the tensile stress $\sigma_{ct,el}$ at the elastic limit would neither show a size nor a shape effect if the estimated values according to the statistical approach are considered. In that case the mean value of all test series would be around $\sigma_{ct,el}$ = 7.9 MPa. However, further test series should be performed in order to verify this conclusion.

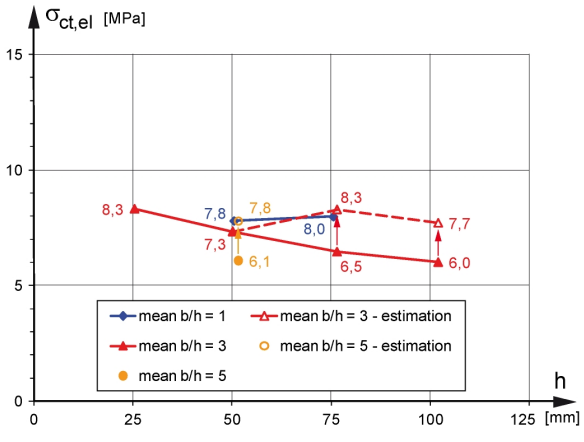

Figure 4: Mean value of elastic limit $\sigma_{ct,el}$ versus height h for different ratios b/h

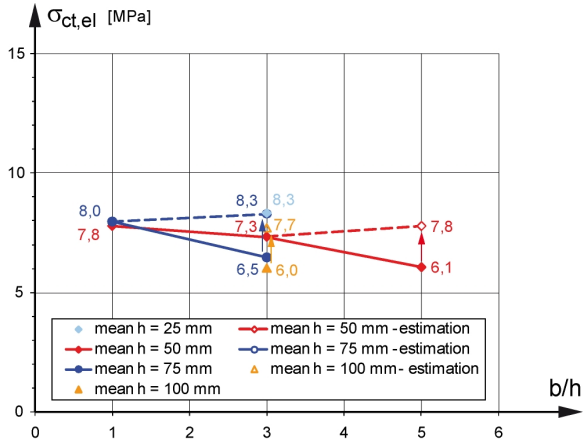

Figure 5: Mean value of elastic limit $\sigma_{ct,el}$ versus ratio b/h for different heights h

2.4 Theoretical Considerations for the tensile strength

The size and shape effect of the tensile strength discovered in tests (Fig. 6) was investigated in detail by Frettlöhr (2011) by using a statistical approach similar to that in section 2.3 as well as considering optical fibre orientation measurements. Additionally the fibre orientation and the fibre density of the specimen cross sections on the tensile strength were measured, but both did not give a clear explanation for the size and shape effect.

The expected tensile strength of the different tensile test series was estimated on basis of the optical measurement of the fibre orientation, fibre diameter and number of fibres. The fibre length based on a random test and the bond strength between the fibres and the concrete matrix was determined to τ_{bf} = 15.8 MPa. Based on this the expected tensile strength was calculated and the comparison with the experimental values showed that the specimens with imperfections did only reach 79 % of the expected tensile strength. The statistical approach showed a similar result that the specimen with imperfections reached only 84 % of the specimen without imperfections.

In Fig. 6 the mean value of the test results (plotted as continuous lines) for the tensile strength f_{ct} of the tests is plotted versus the specimen height h, and in Fig. 7 f_{ct} is plotted versus the shape ratio width to height b/h. For comparison also the estimated tensile strength of the specimen with imperfections are shown as dashed lines.

Considering the estimated tensile strength for the specimen with imperfections, neither Fig. 6 would exhibit a size effect nor Fig. 7 a shape effect. Therefore, the decrease of the tensile strength of some large specimens may have been caused by imperfections. If no size or shape effect on the tensile strength is assumed, the mean tensile strength of all test series would be f_{ct} = 14,7 MPa. However, further test series should be performed in order to verify this conclusion based on estimates for the tensile strength of the specimens with imperfections.

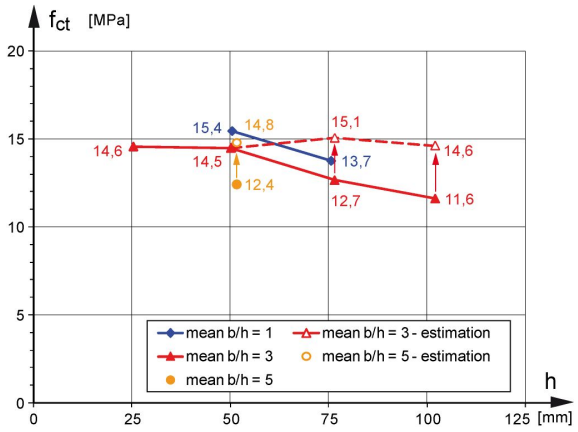

Figure 6: Mean value of tensile strength f_{ct} versus height h for different ratios b/h

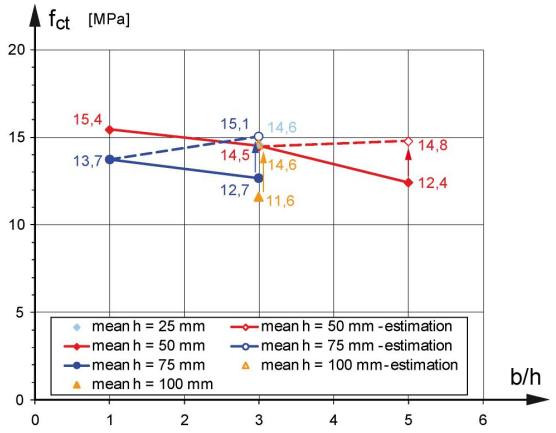

Figure 7: Mean value of tensile strength f_{ct} versus ratio b/h for different heights h

3 SIZE AND SHAPE EFFECT IN BENDING

3.1 Experimental Results

The flexural tensile stress $\sigma_{ctfl,el}$ at the elastic limit is plotted in Fig. 8 versus the depth h of the prisms for both materials tested with different width to height ratios of b/h = 1, 3 and 5. Altogether there is a clear size effect that $\sigma_{ctfl,el}$ decreases with increasing depth h (apart from the prisms with b/h = 5), and the trend lines in Fig. 8 fit well to the test data.

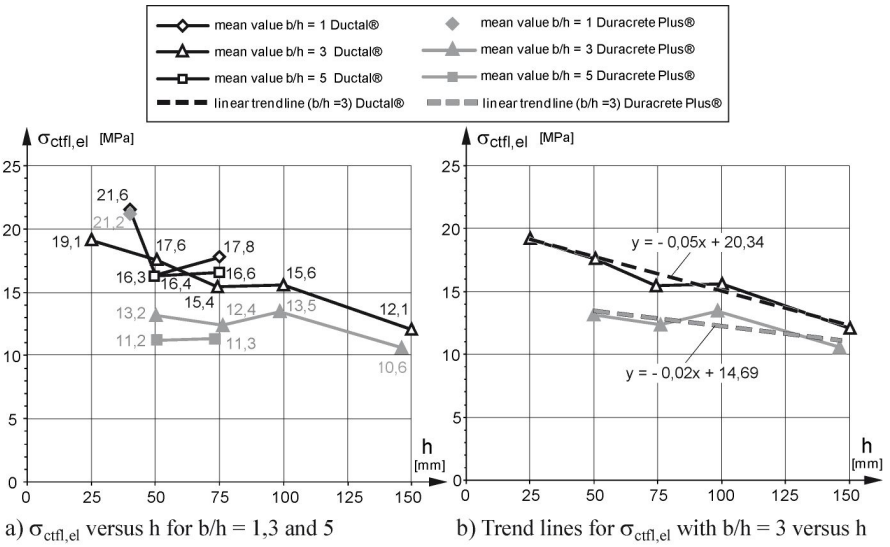

a) $\sigma_{ctfl,el}$ versus h for b/h = 1,3 and 5 b) Trend lines for $\sigma_{ctfl,el}$ with b/h = 3 versus h

Figure 8: Flexural tensile stress $\sigma_{ctfl,el}$ at the elastic limit versus height h for different ratios b/h

For the test series with different values for the ratio b/h the flexural tensile strength $f_{ct,fl}$ is plotted versus the depth h in Fig. 9 for both materials. There is a clear size effect and the decrease of $f_{ct,fl}$ with increasing height h is well predicted by the trend lines shown in Fig. 9.

The shape of the prisms expressed in terms of the ratio b/h appears to play no role for the flexural tensile stress at the elastic limit $\sigma_{ctfl,el}$ as can be seen in Fig. 10. In contrast the flexural tensile strength $f_{ct,fl}$ decreases with increasing ratio b/h and shows a clear shape effect.

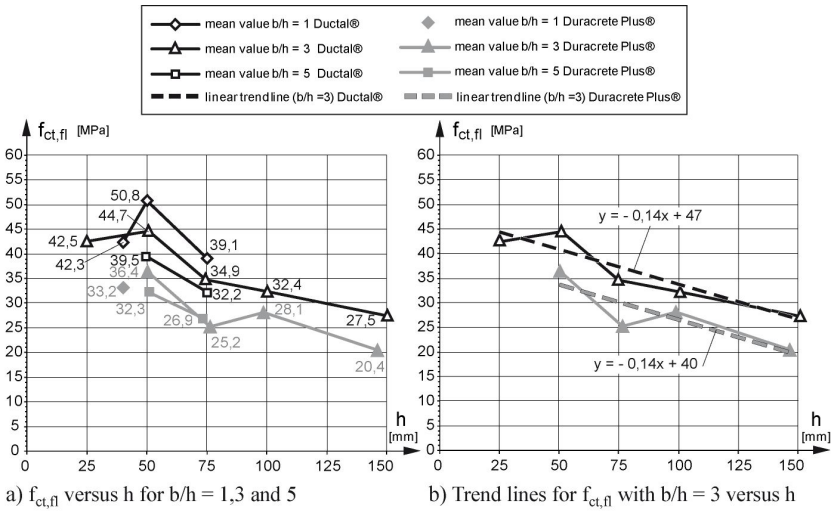

a) $f_{ct,fl}$ versus h for b/h = 1,3 and 5 b) Trend lines for $f_{ct,fl}$ with b/h = 3 versus h

Figure 9: Flexural tensile strength $f_{ct,fl}$ versus height h for different ratios b/h

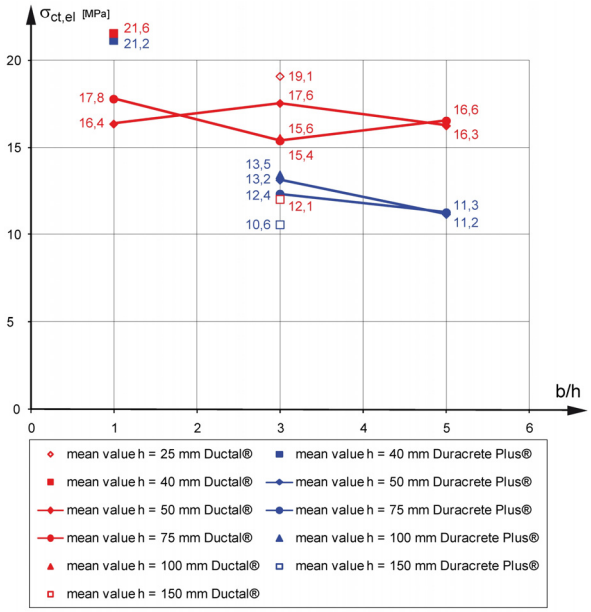

Figure 10: Mean value of flexural tensile stress $\sigma_{ctfl,el}$ at the elastic limit versus ratio b/h for different heights

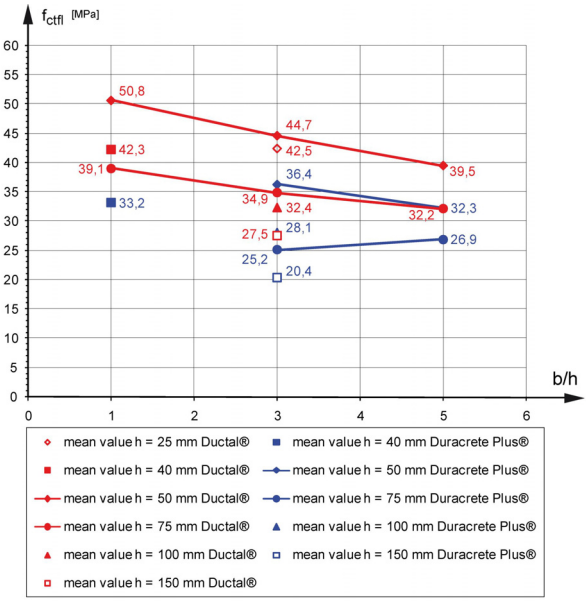

Figure 11: Mean value of flexural tensile strength $f_{ct,fl}$ versus ratio b/h for different heights

3.2 Comparison of elastic limits with proposed relationships

The test results have been compared with the theory by Weibull and an empirical relationship of AFGC/SETRA (2002); details are given by Frettlöhr and Reineck (2009) and Reineck and Frettlöhr (2010, 2011) so that only the conclusions are presented here.

The Weibull modulus m was found not to be constant but decreased with increasing volume from about m = 26 to 12. Contrary to that completely different values of about m = 2 had to be set in order to predict the ratio between the flexural stress to the axial tensile stress of the relevant tests in axial tension. According to AFGC/SETRA (2002) the ratio $\sigma_{ctfl,el}$ /$\sigma_{ct,el}$ between the flexural tensile stress and the axial tensile stress at the elastic limit decreases with an increasing specimen height. However, the test results showed an almost constant ratio. So neither the theory of Weibull nor the relationship of AFGC/SETRA (2002) appear to apply.

3.3 Comparison with a fracture mechanics model considering fibre orientation

The material behaviour in tension of UHPFRC can be divided into an elastic and a crack opening branch followed by a descending branch. A single crack begins to localize at the maximum load. Therefore, based on the „fictitious crack model“ of Hillerborg et al. (1976) and the detailed investigations on fracture mechanics models for normal strength concrete by Reinhardt (1984, 1986), Frettlöhr (2011) developed a fracture mechanics model. He proposed a constitutive law in tension for UHPFRC considering the influence of the fibre orientation. It was shown that the fibre orientation and the tensile strength have a nonlinear relationship. The flexural tensile strength of the test series was calculated using this fracture mechanics model in combination with the proposed constitutive law by Frettlöhr (2011).

The results were compared with tests and the following proposals:

- Model by Casanova and Rossi (1996);
- AFGC/SETRA (2002) recommendation for transforming the stress - crack opening relationship into a stress-strain relation by applying a „structural length“ of $l_{stl} = 2/3 \cdot h$;
- „Structural length“ of $l_{stl} = 2 \cdot (h-x)$ proposed by Fehling and Leutbecher (2011) for transforming the stress - crack opening relationship into a stress-strain relationship.

In Fig. 12 the flexural tensile strength versus the height h for b/h = 3 are compared for the different approaches. The flexural tensile strength of the test series decreases by ~35 % with an increasing specimen height from h = 25 to 150 mm. The approaches of Casanova and Rossi (1996), AFGC/SETRA (2002) and Fehling and Leutbecher (2011) each show a decrease of the flexural tensile strength of only about 12 to 16 % and match the test results for h = 75 respectively 100 mm. However, the model proposed by Frettlöhr (2011) exhibits smaller discrepancies in comparison to the test results; for h = 25, 75, 100 and 150 mm the difference to the test results is only 3 to 7 %. The theoretical flexural tensile strength for h = 50 mm reaches only 81 % of the test value, but this test appears to be an outlier. A comparison of the test series for b/h = 1 and 5 show similar results as described for b/h =3.

In Fig. 13 the mean flexural tensile strengths of the test series with h = 75 mm is plotted versus the ratio b/h and compared with the model proposed by Frettlöhr (2011). For a depth of h = 75 mm the tests exhibited a decrease of the flexural tensile strength from b/h = 1 to 5 of ~17.6 %. The calculated values according to the model decreased by ~13 %, so the deviation is low.

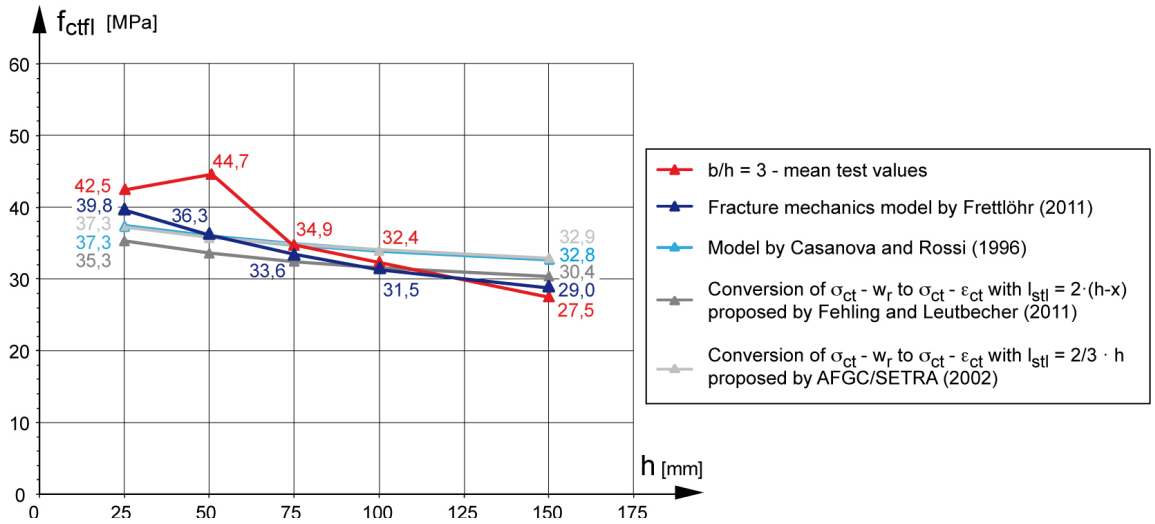

Figure 12: Test results for flexural tensile strength $f_{ct,fl}$ versus height h compared with the different approaches

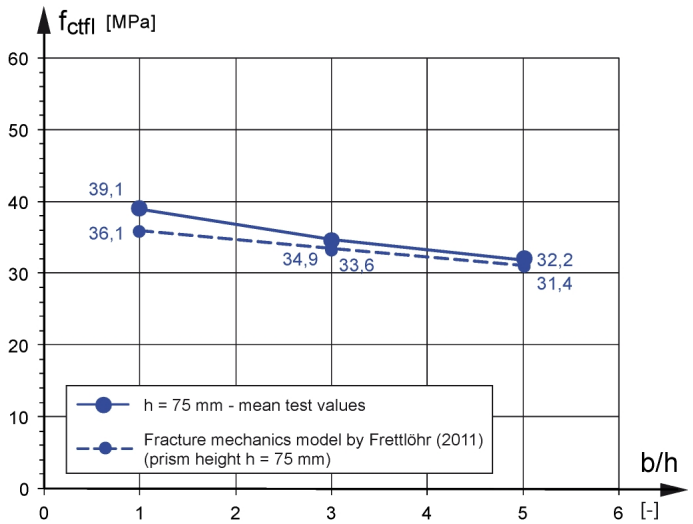

Figure 13: Test results for the flexural tensile strength $f_{ct,fl}$ versus the ratio b/h for prisms with h = 75 mm and comparison with the model proposed by Frettlöhr (2011)

4 CONCLUSIONS

Theoretical considerations based on optical fibre orientation measurements and statistical analyses showed that possibly the imperfections of some specimen with high depths lead to the decrease with increasing height (size effect) of both the elastic limit and the tensile strength of the tests subjected to axial tension. Further test series should be performed in order to verify this. The evaluations of the elastic limits of the flexural stress showed that neither the theory of Weibull nor the empirical relationship of AFGC/SETRA (2002) could explain the size and shape effect of the tests. These effects have to be considered in design and require further research. For UHPFRC in bending the size effect on the flexural tensile strength as well as the influence of the shape need to be considered in design. The fracture mechanics model and the constitutive law in tension proposed by Frettlöhr (2011) consider the influence

of the fibre orientation and give a theoretical explanation for the experimentally determined size and shape influence on the flexural tensile strength.

ACKNOWLEDGEMENTS

The authors are grateful to the Deutsche Forschungsgemeinschaft (DFG), Germany for the grant enabling this research program. The authors also appreciate the support by the firms Lafarge, Paris, Schwenk Zement KG, Ulm, Sebastian Wochner GmbH & Co. KG, Dormettingen and Stratec GmbH, Hemer.

REFERENCES

[1] AFGC/SETRA: Bétons fibrés à ultra-hautes performances. Recommandations provisoires. (Ultra high performance fibre-reinforced concretes) Documents scientifiques et techniques. Association Française de Génie Civil, SETRA, Bagneux Cedex. Janvier 2002, 1-152

[2] Casanova, P.; Rossi, P. (1996): Analysis of metallic fibre-reinforced concrete beams submitted to bending. Material and Structures, Vol. 29, July 1996, 354-361

[3] Fehling, E.; Leutbecher, Th. (2011): Bemessung von Bauteilen aus UHPC. Vortrag am 9. Münchner Baustoffseminar - UHPC, 14. April 2011

[4] Frettlöhr, B; Reineck, K.-H. (2009). Versuche zum Maßstabseinfluss bei kombinierter Beanspruchung aus Biegung und Längskraft von dünnen Bauteilen aus ultrahochfestem Faserfeinkornbeton. Abschlussbericht zum DFG Forschungsvorhaben RE 813/6. Universität Stuttgart, Institut für Leichtbau Entwerfen und Konstruieren (ILEK). September 2009

[5] Frettlöhr, B .; Reineck, K.-H. (2011): Versuche zum Maßstabseinfluss bei Biege- und zentrischer Zugbeanspruchung von UHFFB mit einer Druckfestigkeit von 169 MPa. Bauingenieur 86 (2011), H. 5, 227-232

[6] Frettlöhr, B. (2011): Bemessung von Bauteilen aus ultrahochfestem Faserfeinkornbeton (UHFFB). Diss., Institut für Leichtbau Entwerfen und Konstruieren (ILEK), Universität Stuttgart

[7] Frettlöhr, B.; Reineck, K.-H.; Reinhardt, H.-W. (2012): Size and shape effect of UHPFRC prisms tested under axial tension and bending. 365-372 in: Parra-Montesinos, G.J.; Reinhardt, H.-W.; Naaman, A.E. (Editors) (2012): High performance fiber reinforced cement composites 6, HPFRCC 6. Springer, RILEM 2012, Volume 2, 365 - 372

[8] Hillerborg, A.; Modéer, M.; Petersson, P.-E. (1976): Analysis of crack formation and crack growth in concrte by means of fracture mechanics and Finite Elements. Cement and Concrete Research, Vol. 6 (1997), 783-782

[9] Reineck, K.-H.; Frettlöhr, B. (2010): Tests on scale effect of UHPFRC under bending and axial forces. 3rd fib International Congress 2010, Washington DC. Paper 54. 14 pp.

[10] Reineck, K.-H.; Frettlöhr, B (2011): Versuche zum Maßstabseinfluss bei kombinierter Beanspruchung aus Biegung und Längskraft von UHFFB mit einer Druckfestigkeit von 211 MPa. Bauingenieur 86 (2011), H. 1, 42-52

[11] Reinhardt, H.-W. (1984): Fracture Mechanics of an elastic softening Material like Concrete. HERON, Vol. 29 (1984), No.2, STEVIN-Laboratory of the department of Civil Engineering, Delft University of Technology and Institute TNO for Building Materials and Building Structures, Rijswijk (ZH), Netherlands, 1984, 42 pp.

[12] Reinhardt, H.-W. (1986): The role of fracture mechanics in rational rules for concrete design. IABSE Survey S-34/86 in IABSE Per. 1/1986

[13] Wefer, M. (2010): Materialverhalten und Bemessungswerte von ultrahochfestem Beton unter einaxialer Ermüdungsbeanspruchung. Diss., Institut für Baustoffe, Leibniz Universität Hannover. in: Berichte aus dem Institut für Baustoffe, Heft 7, 2010